Published April 15, 1991

pH-induced Microtubule-dependent Redistribution of Late Endosomes in Neuronal and Epithelial Cells

Robert G. Parton, Carlos G. Dotti, Robert Bacallao,* Ira Kurtz,* Kai Simons, and Kristian Prydz

European Molecular Biology Laboratory, Cell Biology Program, Postfach 10.2209, D-6900 Heidelberg, Federal Republic of Germany; and *Division of Nephrology, University of California Los Angeles Medical Center, Los Angeles, California 90024

Abstract. The interaction between late endocytic structures and microtubules in polarized cells was studied using a procedure previously shown to cause microtubule-dependent redistribution of lysosomes in fibroblasts and macrophages (Heuser, J. 1989. *J. Cell Biol.* 108:855–864). In cultured rat hippocampal neurons, low cytoplasmic pH caused cation-independent mannose-6-phosphate receptor–enriched structures to move out of the cell body and into the processes. In filter grown MDCK cells lowering the cytosolic pH to ~6.5 caused late endosomes to move to the base of the cell and this process was shown to be microtubule dependent. Alkalinization caused a shift in distribution towards the apical pole of the cell. The results are consistent with low pH causing the redistribution of late endosomes towards the plus ends of the microtubules. In MDCK cells the microtubules orientated vertically in the cell may play a role in this process. The shape changes that accompanied the redistribution of the late endosomes in MDCK cells were examined by electron microscopy. On low pH treatment fragmentation of the late endosomes was observed whereas after microtubule depolymerization individual late endosomal structures appeared to fuse together. The late endosomes of the MDCK cell appear to be highly pleomorphic and dependent on microtubules for their form and distribution in the cell.

In fibroblasts, microtubules radiate out from the centrally located microtubule organizing center towards the periphery of the cell. The minus ends of the microtubules are associated with the centrioles while the plus (fast-growing) ends are peripherally located. This organization is important for maintaining the intracellular organization of the membrane-bound compartments of the exocytic and endocytic pathways and for directed membrane traffic between these compartments (for review see Kelly, 1990). On the biosynthetic pathway, the endoplasmic reticulum is extended out along microtubules to the cell periphery (Terasaki et al., 1986) and the involvement of a mechanochemical ATPase, such as kinesin, which drives movement towards the plus ends of the microtubules has been suggested (reviewed by Terasaki, 1990). The Golgi apparatus is maintained in a central position apparently by interaction with minus-end directed motors (Ho et al., 1989). The interactions of both these compartments with microtubules are highly dynamic as shown by observations of living cells (Lee and Chen, 1988; Cooper et al., 1990). On the endocytic pathway, vesicles containing internalized markers move from the cell periphery to the perinuclear region of the cell in a microtubule-dependent fashion (Herman and Albertini, 1984; De Brabander et al., 1988). Possible candidates for these vesicles are large spherical structures, termed endosome carrier vesicles, in which internalized markers accumulate after microtubule depolymerization (Gruenberg et al., 1989). Lysosomes also interact with microtubules and so are maintained in a perinuclear position in the cell (Matteoni and Kreis, 1987). In macrophages, the lysosomes are aligned on microtubules to form long tubules (Swanson et al., 1987; Knapp and Swanson, 1990) and experimentally induced cytosolic acidification causes them to move out along microtubules to the cell periphery (Heuser, 1989).

Polarized cells show specialized microtubule organization. For example, in neuronal cells, which have been extensively studied as a model system for microtubule-dependent movement of organelles (Adams, 1982; Allen et al., 1982; Vale et al., 1985), the microtubules are organized into bundles of uniform polarity (Heidemann et al., 1981). These microtubules mediate the vesicular transport of newly synthesized material from the cell body to the synapses at the tips of the axons whereas material destined for degradation is routed in the opposite direction (reviewed by Grafstein and Forman, 1980). In polarized epithelial cells the microtubule network shows a different organization. The microtubules do not radiate out from a single nucleating center but the majority run vertically through the cell (Gorbsky and Borisy, 1985; Achler et al., 1989; Tucker et al., 1986; Bacallao et al., 1989). The plus ends of the microtubules are predominantly basal while the minus ends are close to the apical surface (Mogen-

K. Prydz's present address is Institute for Cancer Research, The Norwegian Radium Hospital, Montebello, 0310 Oslo 3, Norway.

Published April 15, 1991

sen et al., 1989; Bacallao et al., 1989). In addition, a dense cap of microtubules of mixed polarity lies underneath the apical surface and a sparse network lies at the base of the MDCK cell (Bacallao et al., 1989). The bulk of these microtubules are not organized by the centrioles, which lie directly under the apical surface (Buendia et al., 1990). Microtubules seem to play a role in the maintenance of the polarized phenotype by directing exocytic and endocytic traffic. For example, delivery of exocytic vesicles to the apical surface of epithelial cells appears to be mediated by microtubules (Rindler et al., 1987; Achler et al., 1989; Eilers et al., 1989) and microtubules are involved in endocytic transport from the two sets of early endosomes in the MDCK cell to the late endosomes (Bomsel et al., 1990). The positioning of endocytic organelles in differentiating epithelial cells also appears to involve microtubules (reviewed by Fleming and Johnson, 1988). The role of the vertically orientated microtubules in these processes is at present unclear.

In the present study we examined the interaction of endocytic organelles with microtubules in these two types of polarized cells using cultured rat hippocampal neurons and MDCK epithelial cells. In neurons, low cytoplasmic pH caused a dramatic redistribution of cation-independent mannose-6-phosphate receptor (CI-MPR)[1]-positive late endocytic structures that moved out of the cell body and into the processes. We studied this in more detail in MDCK cells. Late endosomes, and to a partial extent, lysosomes moved to the base of the cells. The Golgi apparatus and early endosomes showed no apparent change in distribution. The late endosomes, but not the lysosomes, also underwent fragmentation at low pH. Movement was shown to be microtubule dependent and towards the plus ends of the microtubules in MDCK cells. On alkalinization the distribution of late endosomes was shifted towards the apical pole of the cell. On microtubule depolymerization, individual late endosomal structures appeared to fuse with each other. These results suggest that under normal conditions the distribution of late endosomes in both these polarized cells is maintained through interactions with microtubules and that they can move retrogradely (apically) or anterogradely (basally) upon manipulating the cytosolic pH.

Materials and Methods

Cell Culture

MDCK. MDCK strain II cells were plated on polycarbonate filters (Transwell 3412; Costar, Cambridge, MA) at low density and maintained in culture for 5 d before use, as described by Bacallao et al. (1989).

Rat Hippocampal Neurons. Hippocampal cultures were prepared as described previously (Banker and Cowan, 1977; Bartlett and Banker, 1984).

Acidification and Alkalinization Media

The following is as described in Heuser, 1989. Ringers' solution: 155 mM NaCl; 5 mM KCl; 2 mM $CaCl_2$; 1 mM $MgCl_2$; 2 mM NaH_2PO_4; 10 mM Hepes pH 7.20; 10 mM glucose; 0.5 mg/ml BSA. Acetate Ringers': as above, with the following changes: 80 mM NaCl, 70 mM Na acetate, 10 mM Hepes, pH as appropriate. Ammonium chloride Ringer's: 20 mM NH_4Cl in normal Ringer's solution (above). All solutions were allowed to equilibrate with air and were warmed to 37°C before use.

1. *Abbreviations used in this paper*: BCECF-AM, 2',7'-biscarboxyethyl 5,6 carboxy-fluorescein acetoxymethyl ester; CI-MPR, cation-independent mannose-6-phosphate receptor; pHi, cytosolic pH.

Optimization of Cytosolic Acidification Conditions

In preliminary experiments the optimal acidification conditions described by Heuser (1989) were used. Acetate Ringers', pH 6.90 (see above), which decreased the cytosolic pH (pHi) to 6.50 in macrophages (Heuser, 1989) consistently produced a redistribution of late endocytic structures in neuronal cells. However, only a partial and somewhat variable effect was observed in MDCK cells. We felt this may reflect the ability of epithelial cells to efficiently regulate their internal pH (Boron, 1986) and so we determined pHi under these conditions as described below. Resting pHi was 7.05 ± 0.15 (mean of three experiments ± SD). Acetate Ringers', pH 6.90, caused a rapid decrease in pHi to ~6.50 but then the pH increased to 6.70 within 2 min (Fig. 3 *a*). We tested the ability of buffers of lower pH to decrease pHi. Acetate Ringers', pH 6.60, quickly lowered pHi to 6.27 (Fig. 3 *b*). After 2 min pHi increased to 6.46 and after 15 min, when the distribution of labeled structures was examined, pHi was 6.57 ± 0.10. The optimal buffer for the redistribution of endocytic structures was found to be acetate Ringer's, pH 6.65. This buffer was therefore used in all subsequent experiments with MDCK cells. Acetate Ringers' pH 6.65 or 6.90 caused similar effects on the distribution of late endocytic structures in neurons.

Fluorescent Measurement of Intracellular pH

pHi was measured as described previously (Kurtz and Golchini, 1987). The fluorescent probe 2',7'-biscarboxyethyl-5,6 carboxyfluorescein acetoxymethyl ester (BCECF-AM) (Molecular Probes Inc., Eugene OR) was used to monitor the pHi (Rink et al., 1982). All experiments were conducted at 37°C. The MDCK cells were grown as described above. The filter was cut out of the holder and immersed in Ringers', pH 7.20, at 37°C for 30 min before the start of the experiment. The filter was cut into two rectangular segments and mounted between two plastic coverslips. The coverslips had a 6 × 9-mm oval hole which allowed free access of buffer to both sides of the filter. The entire assembly was positioned at a 45° angle in plastic cuvettes which were placed into a thermoregulated chamber in an LS-5 fluorometer (Perkin-Elmer Corp., Pomona, CA). The fluorescence emission was monitored at 530 nm and the excitation wavelength was alternated between 500 and 440 nm (isobestic wavelength). Before loading the cells with BCECF, the background intensity at both wavelengths was measured and electronically subtracted from the fluorescence measurements in all experiments. The cells were loaded with 13 μM BCECF-AM for 10 min in the Ringers', pH 7.20 buffer. After the loading period, the filter was washed several times with dye-free Ringers', pH 7.20 and allowed to equilibrate for an additional 5 min in this buffer. The buffer was changed once again and the fluorescence emission was continuously monitored. The Ringers', pH 7.20, was aspirated and replaced with acetate Ringers', pH 6.60 or 6.90. Calibration of intracellular BCECF-AM was performed by monitoring the 500/440 nm excitation ratio at various values of pHi. The pHi was set to the external pH by exposing the cells to a solution containing 130 mM KCl, 20 mM $CaCl_2$, 1 mM $MgCl_2$, 5 mM Hepes, and 1 μM nigericin (Sigma Chemical Co., St. Louis, MO). The resultant calibration curve (the result of three determinations) was used to convert all the fluorescent data to pHi.

Internalization of Endocytic Markers and Acidification/Alkalinization

Horseradish peroxidase (HRP; 10 mg/ml; type II; Sigma Chemical Corp.) was internalized basally in incubation medium (MEM containing 0.2% BSA, 350 mg/liter $NaHCO_3$, and 10 mM Hepes) for 30 min at 37°C. After washing, the cells were reincubated in marker-free medium for 30 min. For the last 10 min of the chase period, the medium was replaced by Ringers' solution, pH 7.20. In some experiments the HRP-containing medium was removed and the filters were immediately immersed in Ringers', pH 7.20. At this stage the filters were usually removed from their holders and cut into pieces. The pieces of filter were then transferred to the different solutions described above for various times at 37°C.

In some experiments, BSA-gold (5 nm, OD_{520} 2–5) was incubated in complete medium basally for 3 h at 37°C and then chased in marker-free medium overnight in order to label lysosomes (i.e., CI-MPR negative, late endocytic structures; Parton et al., 1989).

Lucifer Yellow

Lucifer yellow (dilithium salt; Sigma Chemical Co.) was inactivated as described previously (Bomsel et al., 1989) and internalized at a concentration of 10 mg/ml in glia-conditioned neuronal growth medium (Banker, 1980).

Published April 15, 1991

Electron Microscopy

MDCK cells were embedded in Epon as described previously (Parton et al., 1989) and sectioned perpendicular to the plane of the filter.

Fluorescence Microscopy

Hippocampal cells incubated with inactivated lucifer yellow were fixed in 4% paraformaldehyde/0.25% glutaraldehyde, briefly rinsed in PBS, mounted in PBS/glycerol (1:1) and immediately observed and photographed under a fluorescence microscope (Axiophot; Zeiss).

The intracellular distribution of late endosomal structures after treatment with Ringers' pH 7.20 or acetate Ringers' pH 6.90 (see above) was analyzed by indirect immunofluorescence with a specific antibody raised against the chicken cation-independent mannose-6-phosphate receptor by B. Hoflack and K. Römisch (European Molecular Biology Laboratory, Heidelberg, Federal Republic of Germany) (Parton et al., 1989). After incubation in the appropriate buffer for 15 min the cells were fixed for 6 min in freezing cold methanol. Indirect immunofluorescence was then continued as described previously (Dotti and Simons, 1990).

Microtubule Depolymerization

Endocytic markers were internalized as described above and then the cells were transferred to ice for 30 min. The cells were then incubated in incubation medium containing 33 μM nocodazole (Sigma Chemical Co.) for a further 10 min on ice before being incubated in normal medium, Ringers' 7.20 or acetate Ringers' 6.65 each containing 33 μM nocodazole for various times at 37°C. This procedure has been shown to cause complete microtubule depolymerization as judged by immunofluorescence confocal microscopy (Bacallao, R., and K. Simons, unpublished observations).

Quantitation

The distribution of HRP-labeled structures was quantitated by measuring the relative volume of the labeled structures in arbitrarily defined zones of the MDCK cell as follows (see Table I). Epon-embedded cells were cut perpendicularly to the plane of the filter to generate vertical sections (Baddeley et al., 1986). At least two blocks were sectioned from each experiment and care was taken not to section the same cell more than once by cutting (and discarding) thick sections between the thin sections. Pairs of micrographs

Table I. Distribution and Size of HRP-labeled Endocytic Organelles in MDCK Cells after Treatment with Various Acidification and Alkalinization Media

HRP incubation conditions	Treatment*	Percent of total volume of labeled structures in different regions of the cell‡			Mean structure diameter
		Ap	Bl	Bas	
					μm
30-min incubation and 30-min chase	Ringers' pH 7.20	67	33	21	0.30 ± 0.06
	Acetate Ringers' pH 6.65	27	73	59	0.17 ± 0.04
	Acetate Ringers' pH 6.65, then Ringers' 7.20 10 min	88	12	6	0.20 ± 0.06
	20 mM NH_4Cl	88	12	7	–
	MT-depol§ Ringers' pH 7.20	73	27	10	–
	MT-depol§ acetate Ringers' pH 6.65	83	17	12	–
15-min incubation	Ringers'‖ pH 7.20	72	28	8	–
	Acetate Ringers'‖ pH 6.65	77	23	6	–

* All treatments were for 15 min at 37°C unless otherwise stated.
‡ The volume of HRP-containing structures in each of the three zones of the cell shown diagrammatically below was determined.

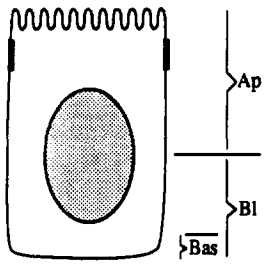

§ Microtubules were depolymerized using cold treatment and then nocodazole as described in Materials and Methods. They were then incubated in the appropriate buffers containing nocodazole.
‖ HRP was internalized for 15 min in the Ringers' or acetate Ringers' to preferentially label the early endosomes.

Published April 15, 1991

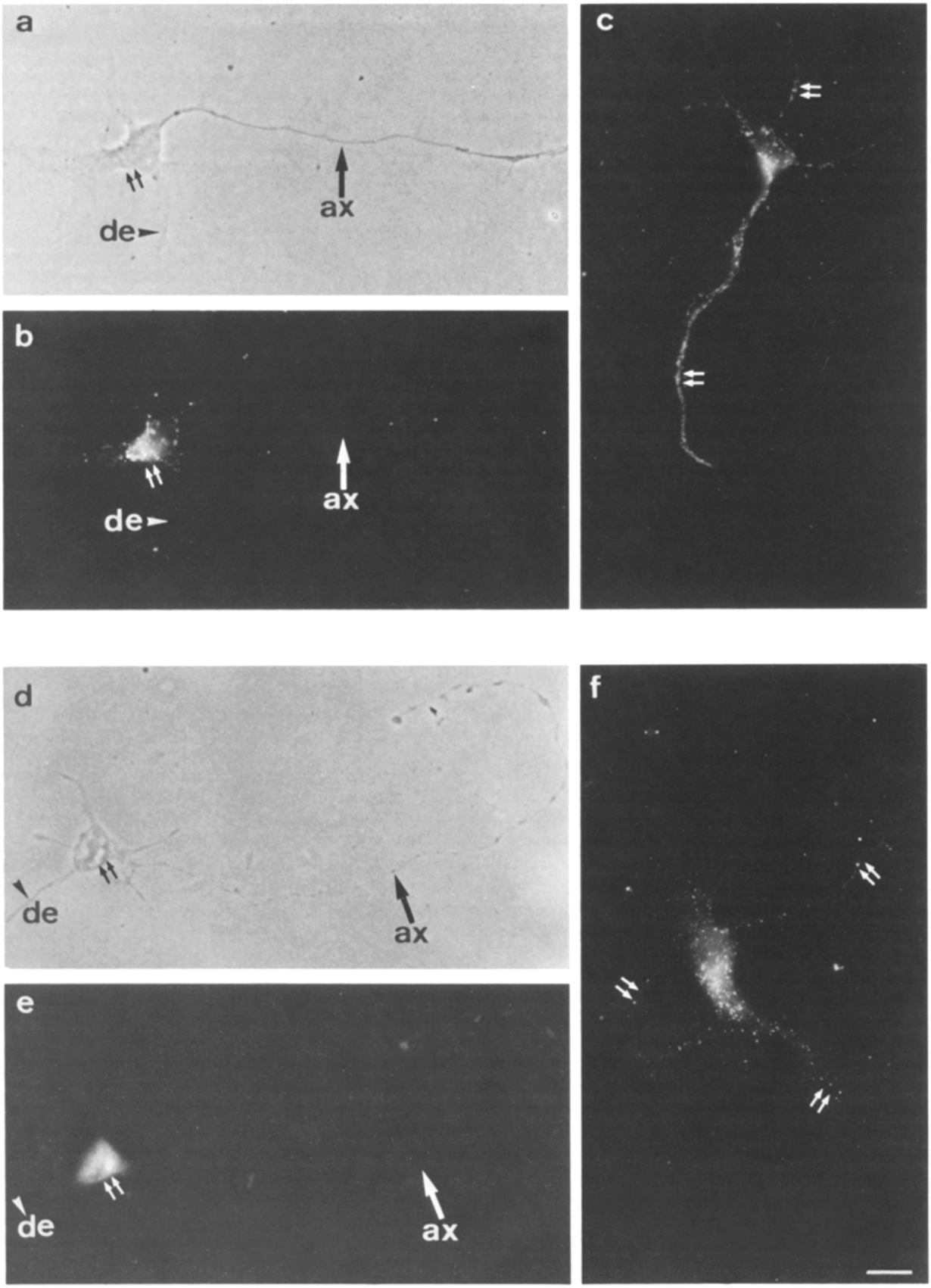

Figure 1. Low pH-induced redistribution of late endocytic structures in rat hippocampal neurons. Stage 3 hippocampal cells were incubated for 30 min in lucifer yellow–containing medium, chased for 30 min in marker-free culture medium, and further incubated for 15 min in Ringers' solution, pH 7.20 (*a* and *b*), or acetate Ringers', pH 6.90 (*c*). Note that at pH 7.20 virtually all the dye is concentrated in the cell body (*double arrows* in *b*). Axons (*ax*, *arrows*) and the minor processes destined to become dendrites (*de*, *arrowheads*) seen in the

Published April 15, 1991

were taken at random along the monolayer at a primary magnification of 10,500. First, the fraction of the cytoplasm occupied by HRP-labeled structures (the total volume density) was estimated by point-counting as described previously (Parton et al., 1989). The volume density was not significantly affected by any of the protocols tested.

We then estimated the volume of the HRP-labeled structures in the apical part of the cell as compared to the basal region, the "midpoint" being defined as the midpoint of the nucleus of the nearest cell. In addition, the relative volume of structures in the most basal 2 μM of the cell was measured. The distribution of lysosomes (BSA-gold containing, HRP-negative structures, see above) was assessed on the same negatives.

To estimate the size of the labeled structures before and after acidification, the diameters of over 150 HRP-labeled profiles were measured (on the same negatives used above). After plotting the data, the graphs were corrected according to Weibel (1979) to compensate for overestimation of mean particle diameter size due to the difficulties in seeing the smallest profiles ("lost caps"). The mean structure diameter and standard error were calculated according to De Hoff (1968) assuming the structures to be spherical.

Results

pH-induced Redistribution of Late Endocytic Structures in Neurons

The neuronal cell is an excellent system to study the microtubule-dependent movement of organelles owing to the spatial separation of the cell bodies and the process tips. Therefore, in initial experiments we examined the effects of low pH on the distribution of late endocytic structures in rat hippocampal neurons. Primary cultures kept for either 3 or 10 d in vitro were used. At the earlier stage (stage 3; see Dotti et al., 1988) the axons and the minor processes destined to become dendrites show the same microtubule polarity with the plus ends at the tips of the processes and the minus ends centrally located (Baas et al., 1989). In contrast, the dendrites of mature cells (stage 5) contain microtubules of mixed polarity (Baas et al., 1988).

Stage 3 cells were incubated with lucifer yellow for 30 min and chased for a further 30 min in marker-free medium in order to label late endocytic structures. The cells were washed in Ringers', pH 7.20 and then reincubated in the same buffer or in acetate Ringers' pH 6.90 for a further 15 min before fixation and analysis by fluorescence microscopy. Control cells kept in Ringers', pH 7.20, contained lucifer yellow almost exclusively in the cell body (Fig. 1 *b*). Only occasionally were punctate structures in the neurites observed. In contrast, after reincubation in acetate Ringers', pH 6.90, punctate staining was evident in both the minor processes and in the axons (Fig. 1 *c*) suggesting that small vesicles had moved out of the cell body. Labeled structures were evident in the tips of processes up to 100 μm long. A similar effect was observed with stage 5 neurons (results not shown). Return of pH-treated cells to Ringers', pH 7.20, caused a return to the control distribution within 15 min.

Antibodies to the CI-MPR have been previously used as markers of the late endosomal compartment (Griffiths et al., 1988; Geuze et al., 1988). We examined the location of CI-MPR in stage 3 hippocampal neurons before and after acidification. Under control conditions labeling was almost exclusively found in the cell body but after acidification labeled structures were evident along the neuronal processes (Fig. 1, *d–f*). These results suggest that low pH induces the movement of CI-MPR-enriched late endosomes out of the cell body.

pH-induced Redistribution of Late Endocytic Structures in MDCK Cells

Further experiments were performed using polarized monolayers of MDCK cells. These cells, like neurons, show a polarized organization of microtubules but their role in cytoplasmic organization is presently unknown. The endocytic pathway in MDCK cells is well-characterized (Bomsel et al., 1989; Parton et al., 1989; Van Deurs et al., 1990; Bomsel et al., 1990) and these cells are amenable to quantitative electron microscopic studies.

Previously we showed that in polarized MDCK strain 1 cells fluid-phase markers internalized from the two surface domains initially entered two distinct sets of peripherally located early endosomes (Parton et al., 1989). After 15 min at 37°C, markers from the two sets of early endosomes then appeared within a single set of late endosomes enriched in the CI-MPR which were shown to be located in the Golgi region of the cell as well as basal to the nucleus. Finally markers entered CI-MPR-negative lysosomes. Using similar incubation conditions with MDCK II cells we labeled late endosomes with HRP (30-min incubation plus 30-min chase) and lysosomes with BSA-gold (3-h incubation with overnight chase) (Fig. 2). As in MDCK I cells, the late endosomes were situated in both the apical and basal regions of the cell whereas the lysosomes generally showed a more apical distribution. We examined the effect of low cytosolic pH on the form and distribution of these structures. The buffer used to decrease the cytosolic pH was acetate Ringers', pH 6.65, which decreased the cytosolic pH to ~6.50 (see Fig. 3 and Materials and Methods).

A 15-min incubation in this buffer caused a dramatic redistribution of HRP-labeled structures (late endosomes; Fig. 4). The labeled structures were now predominantly found in the basal portion of the cell. Clusters of small HRP-labeled vesicles were evident close to the filter and even in basal projections into the filter pores (Fig. 4, *e* and *f*). Few labeled structures were observed in the supranuclear portion of the cells after low pH treatment and no accumulation was ever observed under the apical surface, showing that the low pH conditions did not simply cause a random dispersal of structures to the cell periphery. The gold-labeled HRP-negative lysosomes showed only a partial redistribution to the base of the cell and no differences in morphology were observed (e.g., see Fig. 4 *e*).

corresponding phase contrast micrographs, are almost completely unlabeled. After incubation at pH 6.90 (*c*), lucifer yellow–labeled structures are seen along the cell's processes (*double arrows*). (*d–f*) Immunofluorescence localization of the cation-independent mannose-6-phosphate receptor in stage 3 hippocampal cells. Cells were incubated for 15 min in Ringers', pH 7.20 or acetate Ringers', pH 6.90, fixed and then incubated with an antibody against the CI-MPR. At pH 7.20, the labeling is exclusively located in the cell body (*double arrows* in *e*) whereas at pH 6.90 the labeled structures are also seen along the neurites (*double arrows* in *f*). Exposure times during photography and printing were the same in all the fluorescence micrographs. Bar, 10 μm.

Published April 15, 1991

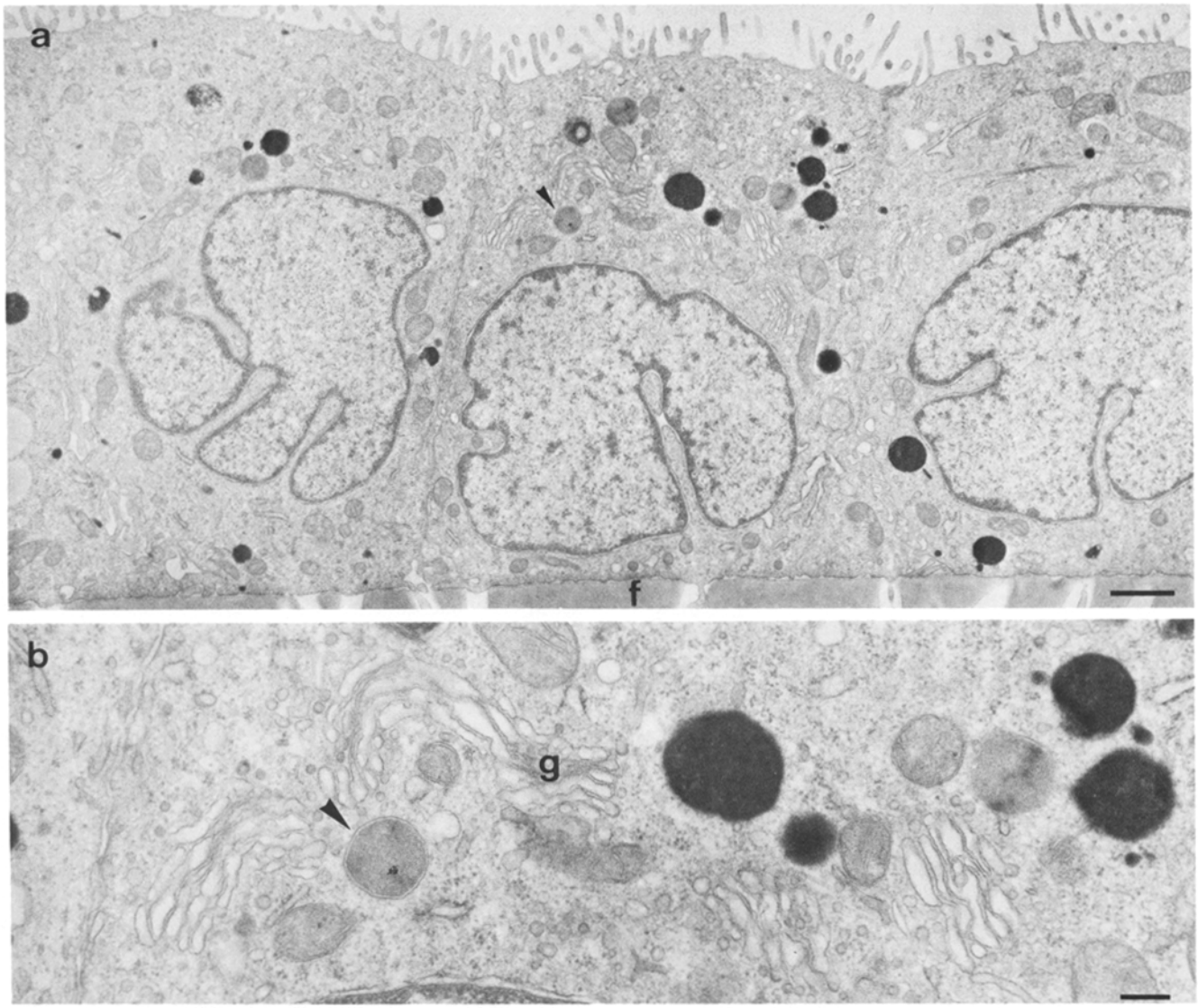

Figure 2. Control distribution of late endosomes and lysosomes in MDCK cells. MDCK cells on filters were incubated for 3 h with 5 nm BSA-gold in the basal medium and then overnight in marker-free medium. They were then incubated for 30 min with HRP in the basal medium and for a further 30 min in marker-free medium. Pieces of the filter were transferred to Ringers' solution, pH 7.20, for 15 min before fixation and processing for EM. HRP labels large vesicular structures, previously shown to be MPR-enriched late endosomes (Parton et al., 1989), which are mainly in the apical part of the cell but are also found basal to the nucleus. A BSA-gold-labeled HRP-negative lysosome (*arrowhead*) with characteristic electron-dense interior is present close to the Golgi apparatus (*g*), also shown at higher magnification in *b*. *f*, filter. Bars: 1 μm (*a*); 0.25 μm (*b*).

To quantitate the effect of pH on the distribution and size of labeled structures, stereological methods were used on random sections cut perpendicular to the basal cell surface (vertical sections). The volume density of the HRP-labeled compartment was not significantly changed upon acidification (1.1 ± 0.3% of the cytoplasmic volume under control conditions; 0.9 ± 0.2% after 15 min at pH 6.65). The volume density of HRP-labeled structures in each of the three zones of the cell shown in Table I was then determined. After a 30-min incubation followed by a 30-min chase, and then reincubation in Ringers' pH 7.20, 67% of the labeled structures were apically located and 33% basal (Table I). Approximately 20% of the labeled structures were found basal to the nucleus. In contrast, after acidification only 27% of the structures were in the apical portion of the cell and 59% of the total were now basal to the nucleus. The percentage of lysosomes in the apical portion of the cell decreased from 70–90 to 30–50%.

We examined the morphological changes that accompanied the movement of the late endosomes (Table I). Under control conditions the mean diameter of labeled structures determined by measurement of over 150 profiles was ~0.30 μm with a maximum profile diameter of 0.90 μM. After the pH 6.65 incubation the number of profiles of smaller diameter had greatly increased. Under these conditions the mean structure diameter was estimated to be 0.17 μm with a maximum of 0.47 μm. Although some small tubular structures were observed at the base of the cell, serial section analysis showed that the bulk of the basally-accumulated structures were individual vesicles and not part of a reticulum under

Published April 15, 1991

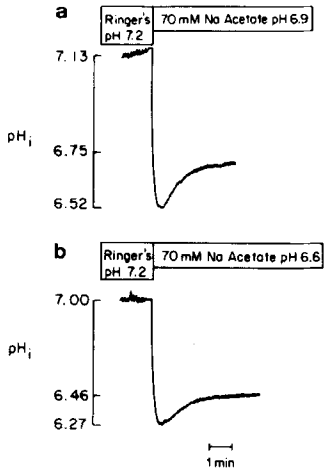

Figure 3. Cytosolic pH measurements in MDCK cells. Filter-grown MDCK cells were incubated with the fluorescent dye BCECF-AM in Ringers', pH 7.20. They were then washed and incubated in the same buffer while monitoring the fluorescence emission at 530 nm. The buffer was replaced with acetate Ringers', pH 6.90 (*a*), or pH 6.60 (*b*).

these conditions (results not shown). This was also evident in thick (0.5 μm) sections (see Fig. 9 *b*).

Next we looked at the reversibility of the basal movement. After removing the low pH medium and reincubation for 10 min in pH 7.20, Ringers', there was a dramatic shift of labeled structures to the apical portion of the cell with very few structures left basal to the nucleus. In many cells a line of vesicles underlying the apical surface was apparent (Fig. 5). Quantitative analysis confirmed that as compared to control conditions more of the labeled structures were apically located with 88% in the apical half of the cell. Many of the labeled structures were of smaller diameter than under control conditions (mean diameter 0.20 μm; Table I). After a further 5–10-min incubation in Ringers', pH 7.20, the control distribution and size of late structures was attained (results not shown).

The shift in the distribution of late endosomes to the apical part of the cell on removal of the low pH medium may be due to the pH increasing above normal as described in mouse macrophages (Heuser, 1989). This was shown to cause a more pronounced central clustering of the endocytic structures in these cells. We therefore looked at the effect of cytosolic alkalinization on the distribution of late endosomes by using NH_4Cl. Incubation of MDCK cells with 20 mM NH_4Cl caused an instant rise in pHi to 7.59 $\pm$ 0.24 (mean $\pm$ SD of three experiments). After 15 min, pHi had decreased to 7.42 $\pm$ 0.21. This treatment caused an apical shift of late endosomes (Fig. 6) with 80% being found apical after a 15-min incubation (Table I). The only morphological change observed after treatment with NH_4Cl was a slight swelling of the HRP-labeled structures. Similar results were obtained with nigericin in Na^+-free medium at pH 7.9 or 8.1 (results not shown).

None of the manipulations caused any obvious change in the general cell morphology or in cell height. In addition, no changes in the microtubule network were evident after immunolabeling low pH-treated cells and observation by confocal microscopy (Bacallao, R., unpublished observations).

Effect of Low pH Medium on the Distribution of Early Endosomes

The above results demonstrate that late endosomes and, to a certain extent lysosomes, of MDCK cells, show pH-dependent apical to basal movement. We investigated whether the early endosomes of these cells were similarly affected by acidification. HRP was internalized from both the apical and basolateral surfaces during a 15-min incubation in acetate Ringers', pH 6.65. Under these conditions the predominant structures labeled were early endosomes with the characteristic morphology described previously (Parton et al., 1989) as well as coated vesicles. The peripheral distribution of the early endosomes in pH 6.65 (Fig. 7) medium appeared exactly the same as previously observed in control cells (Parton et al., 1989; Bomsel et al., 1989). This was confirmed by quantitative analysis of the distribution of early endosomes before and after acidification (Table I). In addition, there was no obvious redistribution of the Golgi complex (e.g., Fig. 4).

Redistribution of Late Endosomes Is Microtubule Dependent

The basal movement of late endosomes on low pH treatment suggests an involvement of the vertically running microtubules of the MDCK cell in the redistribution. We tested this by changing the cytosolic pH after first labeling the late endosomes with HRP, and then inducing microtubule depolymerization using cold treatment and incubation in nocodazole. The apical/basal distribution was identical in cells treated with control medium or with low pH medium (Table I) showing that the redistribution is indeed microtubule dependent. Unexpectedly, however, microtubule depolymerization and reincubation (with or without low pH medium) caused a clustering of the HRP-labeled structures (Fig. 8). Virtually all the labeled structures were in distinct groups which, although predominantly in the apical part of the cell, were also observed basal to the nucleus. This effect was seen after a 15–60-min incubation with medium containing nocodazole after incubation on ice but not immediately after the cold treatment. On removing the nocodazole the clusters became less compact and a normal distribution was attained (results not shown). By serial section analysis of the "clusters" it was evident that many of the apparent vesicles were actually interconnected and this was also supported by observations of thick (0.5 μm) sections (Fig. 9 *c*). Lysosomes (containing BSA-gold but not HRP) also appeared to associate with the clusters, although they did not fuse with the HRP-labeled structures (Fig. 8).

These results suggest that microtubules are important in maintaining the distribution of late endosomes throughout the cell. It has previously been shown that in macrophages lysosomes interact with microtubules to produce long tubules and that conventional fixation caused a breakdown of these tubular structures (Swanson et al., 1987). We therefore examined whether tubular lysosomal profiles can also be visualized in MDCK cells under control conditions. After fixation at 37°C in 2.5% glutaraldehyde as described by Swanson et al. (1987), no extensive tubules were evident even in 0.5-μm sections (see Fig. 9 *a*). Other fixatives such as a recently described paraformaldehyde/cyclohexylamine mixture (Luther and Bloch, 1989) gave similar results (results not shown). Finally, living cells were examined by confocal microscopy after lucifer yellow internalization (Bomsel, M., personal communication). Under control conditions a punc-

Published April 15, 1991

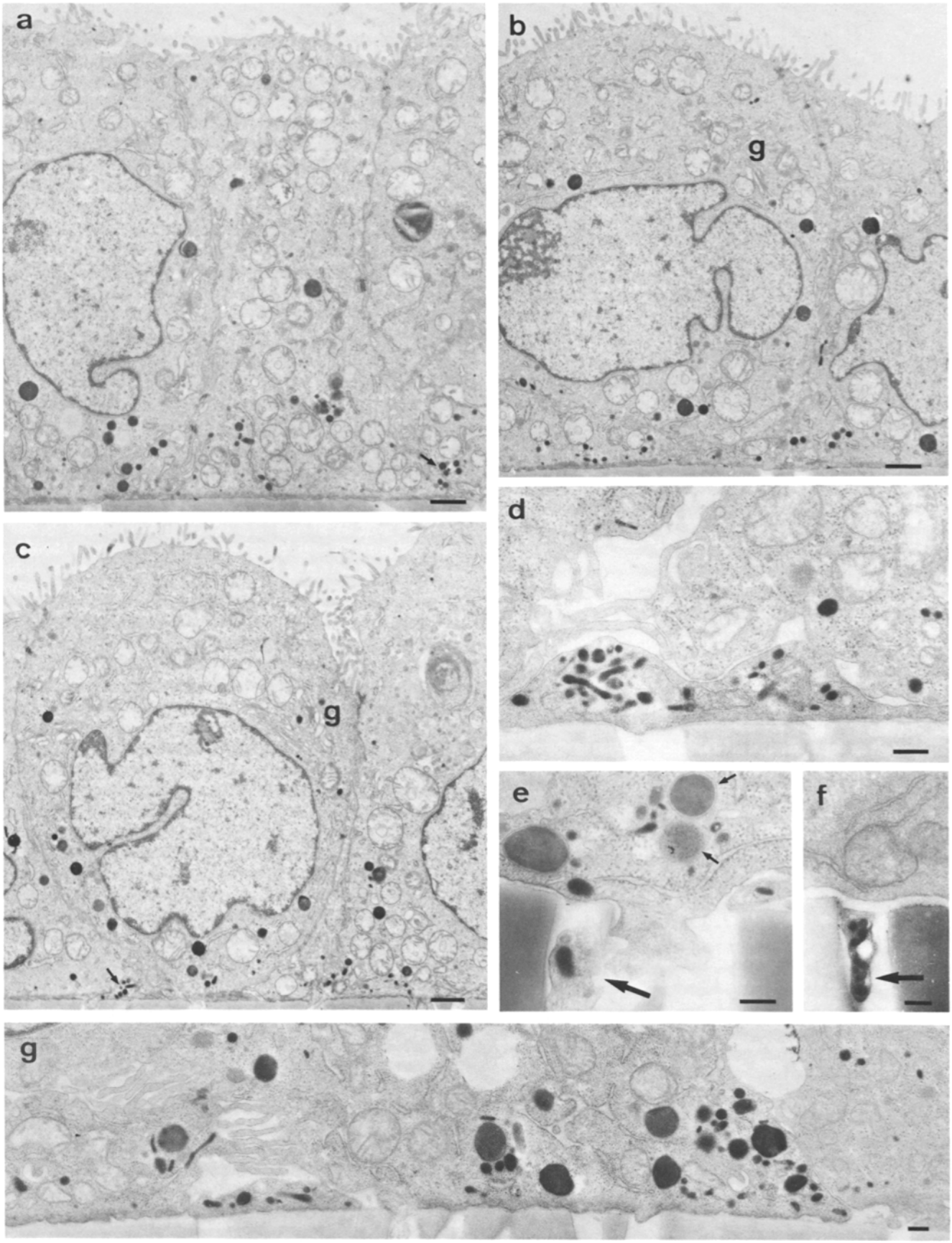

Figure 4. Low pH-induced redistribution of late endosomes in MDCK cells. Late endosomes and lysosomes of filter-grown MDCK cells were labeled as described in the legend to Fig. 2 but pieces of the filter were immersed in acetate Ringers' solution, pH 6.65, rather than Ringers' solution, 7.20. *a*, *b*, and *c* are low magnification images showing the basal accumulation of HRP-labeled late endosomes. Clusters of small vesicles are evident in places (*arrows*). No redistribution of the Golgi apparatus (*g*) is evident. *d*, *e*, *f*, and *g* show higher magnification views of the small vesicles and tubules at the base of the cell. *e* shows lysosomes (*small arrows*) close to the base of the cell and in *e* and *f* HRP-labeled structures are evident in basal projections into the filter (*large arrows*). Note that although the mitochondria appear swollen under these conditions, their morphology returns to normal after removal of the low pH medium (see Fig. 5). Bars: 1 μm (*a–c*); 0.25 μm (*d–g*).

Published April 15, 1991

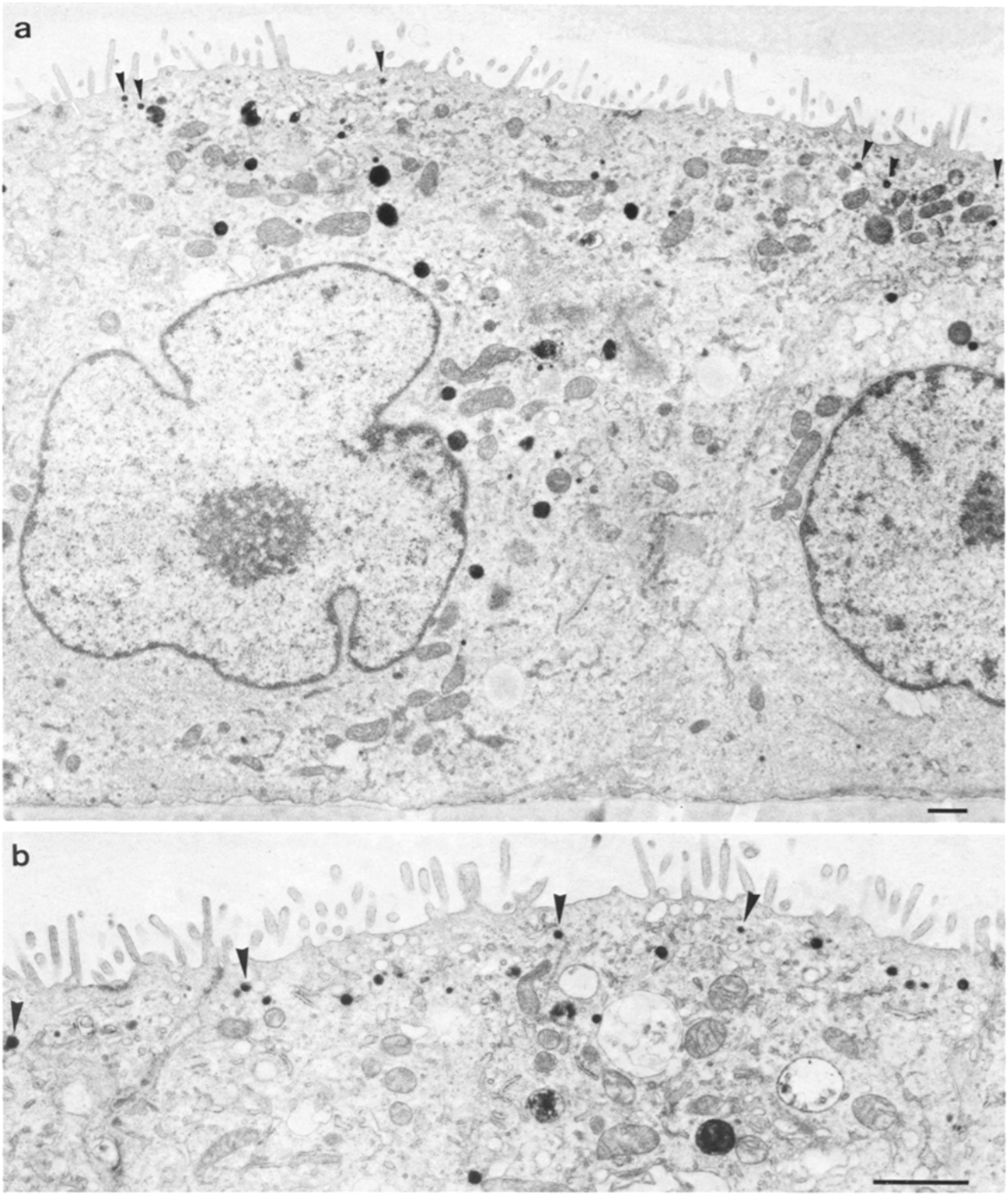

Figure 5. Reincubation of low pH-treated MDCK cells in Ringers', pH 7.20. Cells were treated with low pH medium exactly as described in the legend to Fig. 4 but were reincubated in Ringers' solution, pH 7.20 for 10 min before fixation. Few HRP-labeled structures remain in the basal portion of the cell and in some cells, an example of which is shown at higher magnification in *b*, small vesicles are evident underneath the apical surface (*arrowheads*). Bars, 1 μm.

Published April 15, 1991

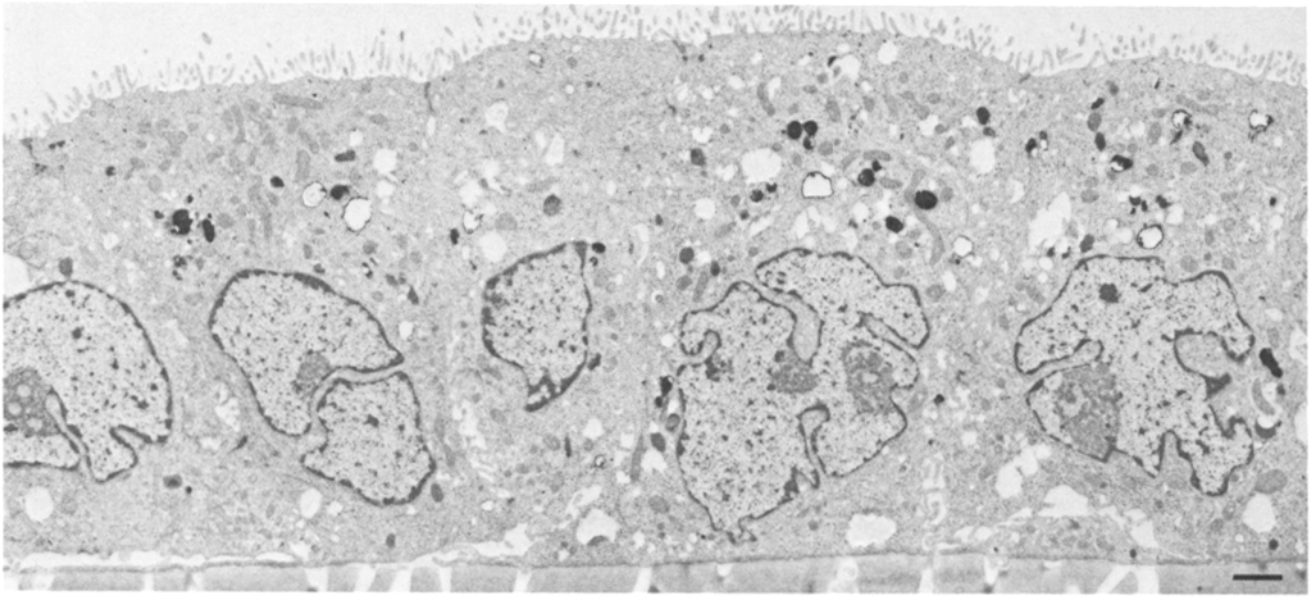

Figure 6. Incubation of MDCK cells in Ringers' solution containing ammonium chloride. Filter-grown cells were incubated with HRP as described in the legend to Fig. 2. Pieces of filter were then incubated for 15 min in Ringers' solution containing 20 mM NH_4Cl before fixation. Few HRP-labeled structures are present in the basal part of the cell. Bar, 1 μm.

tate distribution of label was evident. Late structures were observed both apical and basal to the nucleus. This shows that fixation, which causes a transient lowering of intracellular pH (Johnson, 1985), has no major effect on the distribution or morphology of late endosomes in MDCK cells, although we cannot rule out the presence of narrow tubules between vesicular structures which may be unresolved by these techniques.

Discussion

In this study we examined the interaction of endocytic or-

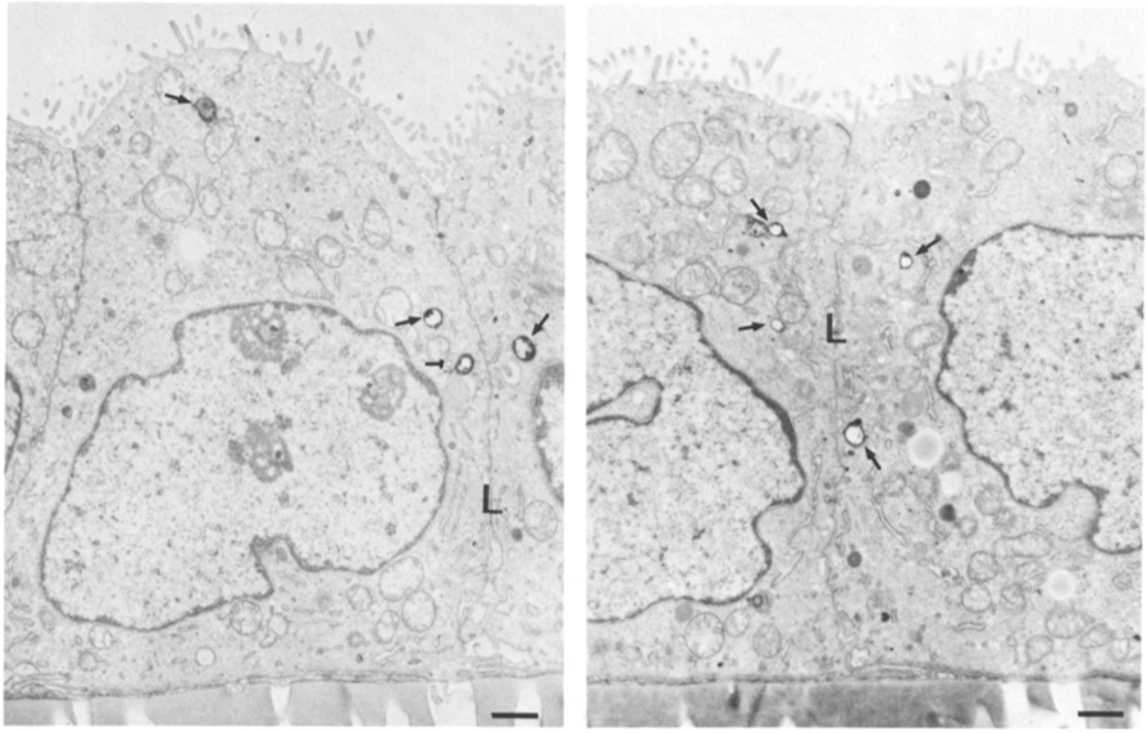

Figure 7. Effect of low pH medium on early endosomes of MDCK cells. MDCK cells were washed for 10 min in Ringers' solution, pH 7.20, and then were incubated with HRP in acetate Ringers', pH 6.65, for 15 min at 37°C. HRP labels structures with the characteristic morphology of early endosomes. These structures are peripherally located in the cell with no evidence of redistribution to the base of the cell. *L*, lateral space. Bar, 1 μm.

Published April 15, 1991

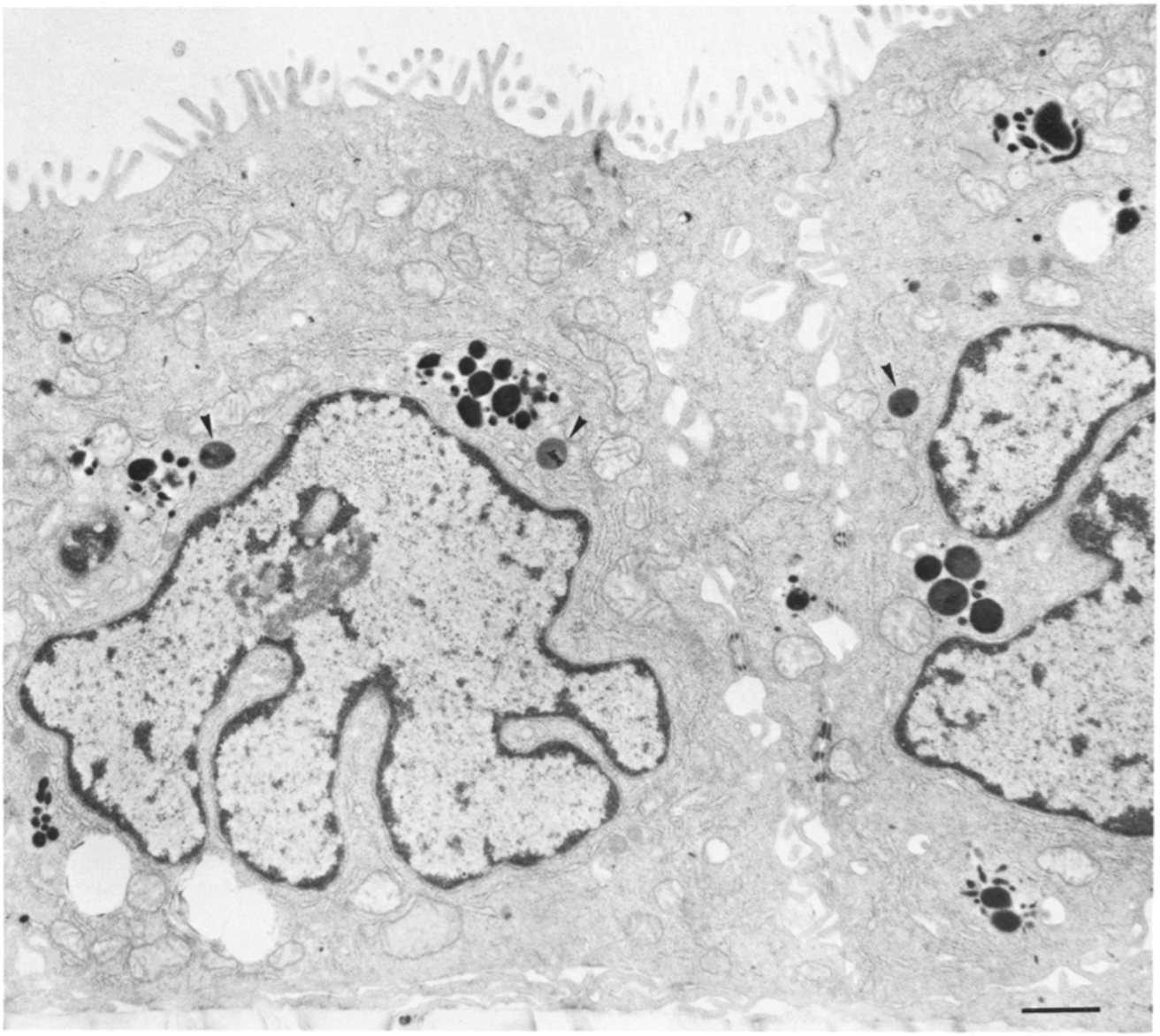

Figure 8. Effect of microtubule depolymerization on the pH-induced redistribution of MDCK cell late endosomes. BSA-gold and HRP were used to label lysosomes and late endosomes, respectively, as described in the legend to Fig. 2. The cells were then incubated at 0°C to induce microtubule depolymerization. Pieces of filter were incubated for 15 min at 37°C in acetate Ringers', pH 6.65, containing 33 μM nocodazole. The late endosomes in the low pH-treated cells have not redistributed to the base of the cell (cf. Fig. 4) showing that the low pH-induced redistribution is indeed microtubule dependent. The late endosomes show different morphology to the control cells (Fig. 2) and have grouped together indicating that under control conditions the distribution of the late endosomes in the cell is dependent on microtubules. Lysosomes (BSA-gold-labeled, HRP-negative structures; *arrowheads*) also sometimes appear to associate with the clusters. Bar, 1 μm.

ganelles with microtubules in two types of polarized cells: neurons and epithelial cells. We used these model systems, in which the organization of the microtubule network is well defined, in order to gain an insight into the role of microtubules in maintaining the distribution and form of endocytic organelles. More specifically, we investigated whether the vertically-running microtubules in epithelial (MDCK) cells play a role in the organization of the endocytic apparatus.

Our results suggest that the form and distribution of late endocytic structures in these cells is maintained through interactions with microtubules. In neuronal cells, late endocytic structures were found to be exclusively located in the cell body. Conditions previously shown to cause plus end-directed movement of lysosomal structures in fibroblasts and macrophages (Heuser, 1989) caused late endocytic structures to move anterogradely out of the cell body and into processes. These results are consistent with the predominant location of the plus ends of the microtubules distal to the cell body (Heidemann et al., 1981). Late endosomal structures were found at the tips of long processes after just 15 min in low pH medium suggesting that fast axonal transport is involved in the redistribution. Removal of the low pH medium caused a rapid retrograde transport back to the cell body suggesting that under physiological pH conditions the late endo-

Published April 15, 1991

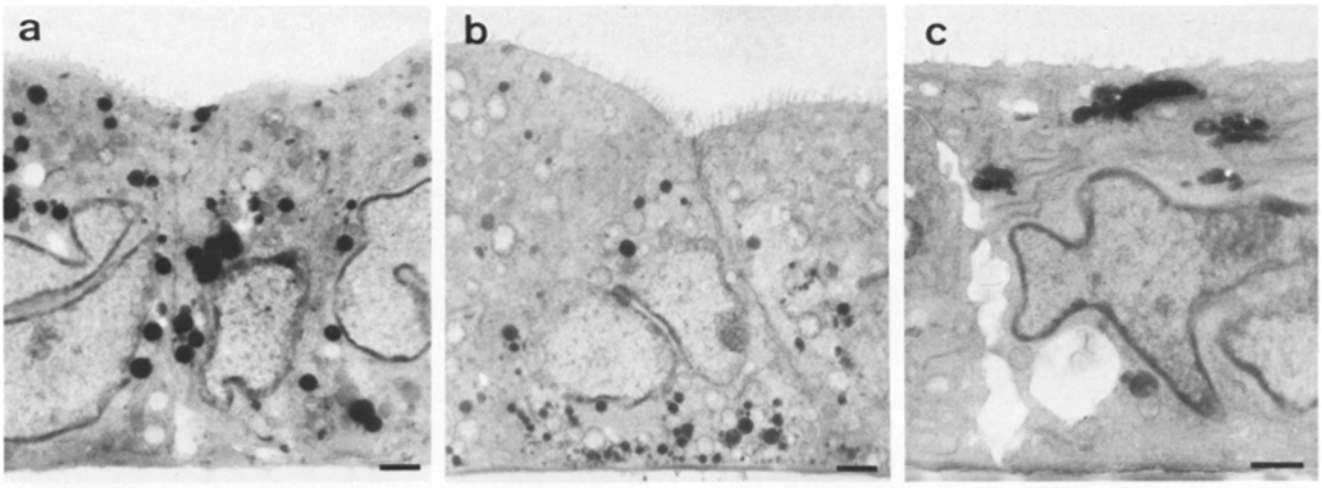

Figure 9. Morphology of late endosomes in thick sections of MDCK cells. (*a*) Control distribution of late endosomes; cells were treated as described in the legend to Fig. 2 but were fixed in 2.5% glutaraldehyde at 37°C as described by Swanson et al. (1987). After processing for EM thick sections (~0.5 μm) were cut and were viewed unstained. HRP labels apparently unconnected vesicular structures dispersed throughout the cell. (*b*) Basal accumulation of late endosomes at low pH; thick sections of cells treated as described in the legend to Fig. 4. Discrete small structures are evident at the base of the cell. (*c*) Distribution of late endosomes in nocodazole-treated cells; thick sections of cells treated as described in the legend to Fig. 8 but incubated in pH 7.20 medium after microtubule depolymerization. Groups of HRP-labeled structures (possibly fused) are evident. Bars, 1 μm.

somes, like the Golgi apparatus, may be maintained in the cell body via minus-end directed transport.

In MDCK cells the late endosomes are distributed throughout the cell under control conditions (Parton et al., 1989, and this study). Lowering the cytosolic pH caused them to accumulate basally suggesting that they interact with the vertically running microtubules that have their plus ends predominantly towards the base of the cell (Bacallao et al., 1989). Consistent with this, alkalinization of the cytosol caused the late endosomes to assume a more apical distribution. Late endosomes moved to within 0.5 μm of the apical or basal surface suggesting that the ends of the microtubules must be very close to the plasma membrane. In *Drosophila* epidermal cells microtubules are attached to the apical and basal surfaces via electron dense attachment sites (Tucker et al., 1986) but no similar structures have so far been observed in MDCK cells. Although the conditions used to induce these changes are nonphysiological, the results suggest that the polarized vertically orientated microtubules in the MDCK cell may have a role in the positioning of the late endosomes in the cell under normal growth conditions. This view is supported by the observation that after microtubule depolymerization the distribution of late endosomes in these cells is altered and individual late endosomal structures associate and fuse with one another. Whether the fused structures are associated with residual segments of incompletely depolymerized microtubules is presently unclear.

The endocytic pathway in MDCK cells has been well characterized (Bomsel et al., 1989; Parton et al., 1989; Van Deurs et al., 1990; Bomsel et al., 1990) and this enabled us to identify the endocytic organelles that showed pH-dependent redistribution. The major effect of the low pH treatment was on the MPR-enriched late endosomes or prelysosomes. These structures also showed a dramatic reorganization after microtubule depolymerization, as described above. The late endosomes appear to form a highly dynamic compartment that is dependent on microtubules for its form and distribution in the cell. It may therefore be analogous to the tubular lysosomes observed in macrophages that form an extensive reticulum spread out on microtubules (Swanson et al., 1987; Knapp and Swanson, 1990). In MDCK cells the predominant form of this compartment appears to be vesicular, rather than tubular, although we cannot rule out the presence of narrow interconnections between apparent vesicles. However, the late endosomes may in fact form one functional compartment so that the endocytic load, and perhaps also lysosomal enzymes and membrane proteins, are distributed throughout all the structures. This is supported by in vitro studies showing that late endocytic structures of MDCK cells (distal to endosome carrier vesicles) mixed their content with an efficiency similar to that of early endosomes (Bomsel et al., 1990). In interspecies cell-fusion experiments, mixing of markers in late endocytic structures was shown to be totally dependent on microtubules (Deng and Storrie, 1988) and recent ultrastructural data suggest that the late endosomes or prelysosomes fuse into a large complex under these conditions (Deng, Y., G. Griffiths, and B. Storrie, manuscript in preparation). Taken together the available evidence suggests that the late endosomes form a dynamic compartment undergoing lateral fusion events that may be facilitated by microtubules.

As previously observed in macrophages, the redistribution of the late endosomes in MDCK cells was accompanied by fragmentation of the compartment. Based on measurements of the mean diameter before and after acidification, our results suggest that one late endosome could form five to six small vesicles on acidification. For this to occur (as the volume of the compartment stayed the same and the surface to volume ratio must increase) there must be recruitment of membrane into the periphery of the vesicles. This may be provided by the internal membranes of the late endosomes. These internal membranes, which are heavily labeled with

Published April 15, 1991

anti-CI-MPR antibodies, are a prominent feature of the late endosomes in MDCK cells (Parton et al., 1989) and other cell types (Griffiths et al., 1988, 1990) and it has been suggested that they are in continuity with the limiting membrane (Griffiths et al., 1988). Consistent with the view that fragmentation involves recruitment of membrane from the interior of the late endosomes, no internal membranes were evident in the small vesicles that accumulated at the base of the cell on low pH treatment (results not shown). The basis of the low pH-induced fragmentation is unclear. It may be a direct effect of low pH or could be related to the redistribution of the late endosomes. Our data tend to support the latter view as the basally accumulated vesicles did not fuse together immediately after washing out the low pH medium but only when the control distribution was attained.

The MPR-negative lysosomes, which under control conditions are mainly apically-located, showed only a partial basal redistribution on lowering the cytosolic pH and no fragmentation was observed. Possibly the optimal experimental conditions required to cause the fragmentation and redistribution of lysosomes are different than those for late endosomes. Alternatively, this may reflect inherent differences in the structure and function of the two organelles. Whereas the late endosomes are highly variable in form, the CI-MPR negative lysosomes in MDCK cells (Parton et al., 1989) as in many other cell types (Alquier et al., 1985; Griffiths et al., 1988) are spherical, electron dense, and of a uniform diameter. In cell fusion experiments lysosomes mixed their content without changing morphology (Deng, Y., G. Griffiths, and B. Storrie, manuscript in preparation). The structures referred to as "residual bodies" in macrophages (Heuser, 1989) may in fact correspond to MPR-negative lysosomes. In the latter study low pH had no significant effect on these structures.

Early endosomes, which are peripherally located in the MDCK cell, showed no change in distribution after low pH treatment (this study) or after microtubule depolymerization (Bomsel et al., 1990). Microtubules do not appear to play a role in delivery of material to this compartment from the cell surface (Gruenberg et al., 1989) or in the in vitro lateral transfer of material between early endosomes (Bomsel et al., 1990). Other cytoskeletal elements may be involved in maintaining the peripheral location of these structures in the MDCK cell.

The mechanism of the pH-induced redistribution of late endosomes is presently unclear. Further experiments in vivo and in vitro are required to determine whether the pH effects are direct (by modulation of motor activity) or indirect. The results are consistent with cytosolic pH causing the modulation of the activity and direction of a single motor or of the involvement of two different microtubule motors, such as kinesin and cytoplasmic dynein, in the redistribution. The clustering of endocytic structures around the microtubule organizing center of fibroblasts (Matteoni and Kreis, 1987) may be mediated by a minus end-directed motor such as cytoplasmic dynein whereas in macrophages the extension of tubular lysosomes along microtubules was shown to involve kinesin (Hollenbeck and Swanson, 1990). In the present study neuronal late endosomes moved anterogradely into axons suggesting the involvement of kinesin in the plus-end directed movement (Vale, 1987). In MDCK cells, the involvement of both cytoplasmic dynein and kinesin in the microtubule-dependent transport steps from the apical and basolateral early endosomes to the single set of late endosomes has been shown (Bomsel et al., 1990). A model was proposed in which endosome carrier vesicles derived from the apical early endosomes moved in the basal direction on the vertically-running microtubules using kinesin whereas basolaterally derived carrier vesicles moved in the opposite direction via dynein; both would then fuse with late endosomes. The late endosomes may interact with microtubules via both these motors and this would be consistent with our observations of microtubule-dependent movement towards both the plus and minus ends of microtubules in MDCK cells. During cytosolic acidification kinesin activity would be favored over dynein (possibly through an indirect effect) and the late endosomes would move basally (and in neurons anterogradely). Consistent with this hypothesis, under control conditions the late endosomes of MDCK cells are not clustered under the apical surface at the minus-ends of the microtubule bundles but are spread throughout the cell. Their position may be maintained by an interplay between kinesin and cytoplasmic dynein. The interactions between organelles, motors, and microtubules and the regulation of motor activity are fundamental to understanding microtubule-dependent membrane traffic. The systems described here may prove to be useful in understanding the mechanisms involved.

We are particularly grateful to Drs. Gareth Griffiths and Jean Gruenberg for their advice throughout the study and comments on the manuscript. We would also like to thank Drs. Morgane Bomsel and Thomas Kreis for their comments on the manuscript, Dr. John Heuser for helpful discussions, and Liane Meyn for help in preparing the hippocampal neuron cultures.

R. G. Parton was supported by a long-term European Molecular Biology organization fellowship; C. G. Dotti was a recipient of an Alexander von Humboldt Stiftung fellowship; K. Prydz was a recipient of a long-term fellowship from the National Council of Science and Humanities, Norway. The work was supported by the National Institutes of Diabetes and Digestive and Kidney Diseases (NIDDK) grant DK-39212 (to I. Kurtz) and the Whitaker Foundation Grant A871013 (to I. Kurtz). I. Kurtz is supported by an American Heart Association Established Investigator Award 900206. R. Bacallao is a recipient of an NIDDK Physician Scientist Award DK-01777.

Received for publication 11 October 1990 and in revised form 27 December 1990.

References

Achler, C., D. Filmer, C. Merte, and D. Drenckhahn. 1989. Role of microtubules in polarized delivery of apical membrane proteins to the brush border of the epithelium. *J. Cell Biol.* 109:179–189.

Adams, R. J. 1982. Organelle movements in axons depend on ATP. *Nature (Lond.).* 297:327–329.

Allen, R. D., J. Metuzals, I. Tasaki, S. T. Brady, and S. P. Gilbert. 1982. Fast axonal transport in squid axon. *Science (Wash. DC).* 218:1127–1128.

Alquier, C., P. Guenin, Y. Munari-Silem, C. Audebet, and B. Rousset. 1985. Isolation of pig thyroid lysosomes. Biochemical and morphological characterization. *Biochem. J.* 232:529–537.

Baas, P. W., J. S. Deitch, M. M. Black, and G. A. Banker. 1988. Polarity orientation of microtubules in hippocampal neurons: uniformity in the axon and nonuniformity in the dendrite. *Proc. Natl. Acad. Sci. USA.* 85:8335–8339.

Baas, P. W., M. M. Black, and G. A. Banker. 1989. Changes in microtubule polarity orientation during the development of hippocampal neurons in culture. *J. Cell Biol.* 109:3085–3094.

Bacallao, R., C. Antony, C. Dotti, E. Karsenti, E. H. K. Stelzer, and K. Simons. 1989. The subcellular organization of Madin-Darby canine kidney cells during the formation of a polarized epithelium. *J. Cell Biol.* 109:2817–2832.

Baddeley, A. J., H. J. G. Gundersen, and L. M. Cruz-Orive. 1986. Estimation of surface areas from vertical sections. *J. Microsc. (Oxf.).* 142:259–276.

Banker, G. 1980. Trophic interactions between astroglial cells and hippocampal

neurons in culture. *Science (Wash. DC).* 209:809–810.
Banker, G., and W. M. Cowan. 1977. Rat hippocampal neurons in dispersed cell culture. *Brain Res.* 126:397–425.
Bartlett, W. P., and G. A. Banker. 1984. An electron microscopic study of the development of axons and dendrites by hippocampal neurons in culture. I. Cells which develop without intercellular contacts. *J. Neurosci.* 4:1944–1953.
Bomsel, M., K. Prydz, R. G. Parton, J. Gruenberg, and K. Simons. 1989. Endocytosis in filter-grown Madin–Darby canine kidney cells. *J. Cell Biol.* 109:3243–3258.
Bomsel, M., R. G. Parton, S. A. Kuznetsov, T. A. Schroer, and J. Gruenberg. 1990. Microtubule- and motor-dependent fusion in vitro between apical and basolateral endocytic vesicles from MDCK cells. *Cell.* 62:719–731.
Boron, W. F. 1986. Intracellular pH regulation in epithelial cells. *Annu. Rev. Physiol.* 48:377–388.
Buendia, B., M. H. Bré, G. Griffiths, and E. Karsenti. 1990. Cytoskeletal control of centrioles movement during the establishment of polarity in Madin–Darby canine kidney cells. *J. Cell Biol.* 110:1123–1135.
Cooper, M. S., A. H. Cornell-Bell, A Chernjavsky, J. W. Dani, and S. J. Smith. 1990. Tubulovesicular processes emerge from trans-Golgi cisternae, extend along microtubules, and interlink adjacent trans-Golgi elements into a reticulum. *Cell.* 61:135–145.
De Brabander, M., R. Nuydens, H. Geerts, and C. R. Hopkins. 1988. Dynamic behaviour of the transferrin receptor followed in living epidermoid carcinoma (A431) cells with nanovid microscopy. *Cell Motil. Cytoskel.* 9:30–47.
De Hoff, R. T. 1968. The estimation of particle-size distribution from simple counting measurements made on random plane sections. *In* Quantitative Microscopy. R. T. De Hoff and F. N. Rhines, editors. McGraw-Hill Inc., New York. 136, 143.
Deng, Y., and B. Storrie. 1988. Animal cell lysosomes rapidly exchange membrane proteins. *Proc. Natl. Acad. Sci. USA.* 85:3860–3864.
Dotti, C. G., and K. Simons. 1990. Polarized sorting of viral glycoproteins to the axon and dendrites of hippocampal neurons in culture. *Cell.* 62:63–72.
Dotti, C. G., C. A. Sullivan, and G. A. Banker. 1988. The establishment of polarity by hippocampal neurons in culture. *J. Neurosci.* 8:1454–1468.
Eilers, U., J. Klumperman, and H.-P. Hauri. 1989. Nocodazole, a microtubule-active drug, interferes with apical protein delivery in cultured intestinal epithelial cells (Caco-2). *J. Cell Biol.* 108:13–22.
Fleming, T. P., and M. H. Johnson. 1988. From egg to epithelium. *Annu. Rev. Cell Biol.* 4:459–485.
Geuze, H. J., W. Stoorvogel, G. J. Strous, J. W. Slot, J. E. Bleekemolen, and I. Mellman. 1988. Sorting of mannose-6-phosphate receptors and lysosomal membrane proteins in endocytic vesicles. *J. Cell Biol.* 107:2491–2501.
Gorbsky, G., and G. G. Borisy. 1985. Microtubule distribution in cultured cells and intact tissues: improved immunolabeling resolution through the use of reversible embedment cytochemistry. *Proc. Natl. Acad. Sci. USA.* 82:6889–6893.
Grafstein, B., and D. S. Forman. 1980. Intracellular transport in neurons. *Physiol. Rev.* 60:1167–1283.
Griffiths, G., B. Hoflack, K. Simons, I. Mellman, and S. Kornfeld. 1988. The mannose-6-phosphate receptor and the biogenesis of lysosomes. *Cell.* 52:329–341.
Griffiths, G., R. Matteoni, R. Back, and B. Hoflack. 1990. Characterization of the cation-independent mannose-6-phosphate receptor-enriched prelysosomal compartment. *J. Cell Sci.* 95:441–461.
Gruenberg, J., G. Griffiths, and K. E. Howell. 1989. Characterization of the early endosome and putative endocytic carrier vesicles in vivo and with an assay of vesicle function in vitro. *J. Cell Biol.* 108:1301–1316.
Heidemann, S. R., J. M. Landers, and M. A. Hamborg. 1981. Polarity orientation of axonal microtubules. *J. Cell Biol.* 91:661–665.
Herman, B., and D. F. Albertini. 1984. A time-lapse video image intensification analysis of cytoplasmic organelle movements during endosome translocation. *J. Cell Biol.* 98:565–576.
Heuser, J. 1989. Changes in lysosome shape and distribution correlated with changes in cytoplasmic pH. *J. Cell Biol.* 108:855–864.
Ho, W. C., V. J. Allan, G. van Meer, E. G. Berger, and T. E. Kreis. 1989. Reclustering of scattered Golgi elements occurs along microtubules. *Eur. J. Cell Biol.* 48:250–263.
Hollenbeck, P. J., and J. A. Swanson. 1990. Radial extension of macrophage tubular lysosomes supported by kinesin. *Nature (Lond.).* 346:864–866.
Johnson, T. J. A. 1985. Aldehyde fixatives: quantification of acid-producing reactions. *J. Electron Microsc. Techn.* 2:129–138.
Kelly, R. B. 1990. Microtubules, membrane traffic and cell organization. *Cell.* 61:5–7.
Knapp, P. E., and J. A. Swanson. 1990. Plasticity of the tubular lysosomal compartment in macrophages. *J. Cell Sci.* 95:433–439.
Kurtz, I., and K. Golchini. 1987. Na^+-independent Cl^--$HCO3^-$ exchange in Madin-Darby canine kidney cells. *J. Biol. Chem.* 262:4516–4520.
Lee, C., and L. B. Chen. 1988. Dynamic behaviour of endoplasmic reticulum in living cells. *Cell.* 54:37–46.
Luther, P. W., and R. J. Bloch. 1989. Formaldehyde-amine fixatives for immunocytochemistry of cultured *Xenopus* myocytes. *J. Histochem. Cytochem.* 37:75–82.
Matteoni, R., and T. E. Kreis. 1987. Translocation and clustering of endosomes and lysosomes depends on microtubules. *J. Cell Biol.* 105:1253–1265.
Mogensen, M. M., J. B. Tucker, and H. Stebbings. 1989. Microtubule polarities indicate that nucleation and capture of microtubules occurs at cell surfaces in *Drosophila. J. Cell Biol.* 108:1445–1452.
Parton, R. G., K. Prydz, M. Bomsel, K. Simons, and G. Griffiths. 1989. Meeting of the apical and basolateral endocytic pathways of the Madin–Darby canine kidney cell in late endosomes. *J. Cell Biol.* 109:3259–3272.
Rindler, M. J., I. Ivanov, and D. D. Sabatini. 1987. Microtubule-acting drugs lead to the nonpolarized delivery of the influenza hemagglutinin to the cell surface of polarized Madin–Darby canine kidney cells. *J. Cell Biol.* 104:231–241.
Rink, T. J., R. Y. Tsien, and T. Pozzan. 1982. Cytoplasmic pH and free Mg^{2+} in lymphocytes. *J. Cell Biol.* 95:189–196.
Swanson, J. A., A. Bushnell, and S. C. Silverstein. 1987. Tubular lysosome morphology and distribution within macrophages depend on the integrity of cytoplasmic microtubules. *Proc. Natl. Acad. Sci. USA.* 84:1921–1925.
Terasaki, M. 1990. Recent progress on structural interactions of the endoplasmic reticulum. *Cell Motil. Cytoskel.* 15:71–75.
Terasaki, M., L. B. Chen, and K. Fujiwara. 1986. Microtubules and the endoplasmic reticulum are highly interdependent structures. *J. Cell Biol.* 103:1557–1568.
Tucker, J. B., M. J. Milner, D. A. Currie, J. A. Muir, D. A. Forrest, and M. J. Spencer. 1986. Centrosomal microtubule organizing centers and a switch in the control of protofilament number for cell surface-associated microtubules during Drosophila wing morphogenesis. *Eur. J. Cell Biol.* 41:279–289.
Vale, R. D. 1987. Intracellular transport using microtubule-based motors. *Annu. Rev. Cell Biol.* 3:347–378.
Vale, R. D., T. S. Reese, and M. P. Scheetz. 1985. Identification of novel force-generating protein, kinesin, involved in microtubule-based motility. *Cell.* 42:39–50.
Van Deurs, B., S. H. Hansen, O. W. Petersen, E. L. Melby, and K. Sandvig. 1990. Endocytosis, intracellular transport and transcytosis of the toxic protein ricin by a polarized epithelium. *Eur. J. Cell. Biol.* 51:96–109.
Weibel, E. R. 1979. Stereological Methods. Vol. 1. Practical Methods for Biological Morphometry. Academic Press, Inc., New York.